EXPERIMENTAL AND NUMERICAL INVESTIGATION OF TIP CLEARANCE NOISE OF AN AXIAL FAN USING A LATTICE BOLTZMANN METHOD

Tao ZHU, Thomas H. CAROLUS

UNIVERSITY OF SIEGEN, Institute for Fluid- and Thermodynamics
Paul-Bonatz-Strasse 9-11, D-57068 Siegen, GERMANY

SUMMARY

The secondary flow through the tip clearance is one of the well-known sources contributing to the overall noise of axial fans. Aerodynamic losses and sound radiation increase significantly as the tip clearance is increased. The objective of this study is to revisit the mechanisms for tip clearance noise from a rotating fan impeller.

The unsteady and compressible numerical Lattice-Boltzmann-Method (LBM) is utilized which allows a direct and simultaneous prediction of both aerodynamic and acoustic field. Overall aerodynamic and acoustic fan performance data as predicted with the LBM were validated with experimental data. The agreement was quite satisfactory which justified looking at the LBM-predicted field data in detail. The flow and acoustic field in the vicinity of an axial fan impeller's tip gap revealed important details of the sound generating mechanism. A large tip clearance is responsible for a complex vortex system with a considerable degree of inherent unsteadiness. The consequences are fluctuations of static pressure in the flow field in the adjacent tip region and on the blade surfaces. Those pressure fluctuations generate sound that is then radiated away from the complete impeller upstream into the free field with the typical hemispherical directivity pattern. At the part load operating point sound pressure level increase in both broad and narrow frequency band were observed, which could be attributed to the complex tip clearance flow.

INTRODUCTION

The aerodynamic and aeroacoustic performance of axial fans are strongly affected by the unavoidable tip clearance. Aerodynamic losses and sound radiation increase significantly as the tip clearance is increased. Tip clearance studies have a long history. Longhouse[1] reported increased broadband noise level as result of an enlarged tip clearance. He focused on the interaction of the tip vortex with the blade tip region, but without a quantitative flow analysis. You et al.[2] illustrated the

complex tip vortex structures as obtained from a Large Eddy Simulation (LES) of a blade cascade with moving wall in a stationary system, including the dominant tip leakage vortex (TLV), the tip separation vortex (TSV) and other induced small scale vortices. The effect of the size of the tip clearance on generation and evolution of vortices was also discussed by You et al.[3]. Fukano and Jang[4] analyzed the tip clearance flow utilizing two hot-wire probes in the rotating blade passage. They proved that the noise due to tip clearance flow was linked to velocity fluctuations in the blade passage. A detailed aeroacoustic investigation of an isolated stationary airfoil placed adjacent to a wall with a well defined gap was carried out by Grilliat et al.[5] and Jacob et al.[6]. They measured pressure fluctuations on the airfoil surface, flow velocities and the flow induced near and far field acoustics. Eventually they identified two mechanisms of tip leakage broadband self noise. A detail experimental study on a low Mach number axial fan was carried out by Kameier and Neise[7] and März et al.[8]: Large tip clearances and high blade loading caused a narrow-band spectral hump in the noise signature which was attributed to rotating flow instability in the gap region. Neuhaus and Neise[9] tried to control tip clearance noise by active flow control, and more recently, Corsini et al.[10] and Aktürk and Camci[11], [12] by passive devices such as tip end-plates and squealers.

The objective of this study is to revisit the mechanisms for tip clearance noise from a rotating fan impeller. Aerodynamic and acoustic measurements are compared with numerical results from an unsteady compressible numerical Lattice Boltzmann method (LBM). As compared to the more classical approach where unsteady flow field data from an unsteady Reynolds averaged Navier-Stokes and/or large eddy simulation are fed into an acoustic Ffowcs Williams and Hawkings (FWH) analogy (see e.g. Zhu and Carolus[13], Moreau[14], Magne[15]), the LBM promises a direct and simultaneous prediction of acoustic field. It is of interest, how LBM-data compare to experimental results and how the LBM-method may foster the understanding of tip clearance noise. Extended from Zhu et al[16] is one more operating point in the part load range investigated in this study.

FANS INVESTIGATED AND TEST RIG

Impellers investigated

An axial fan impeller, Figure 1 (left), was designed with an in-house blade element momentum based design code for low pressure axial fans (dAX-LP, see Carolus[17]). Differently from a free vortex design, the design blade loading is 70% at hub and 120% at tip, distributed approx. linearly in spanwise direction. The loading of the blade tip is done intentionally to provoke strong secondary tip flow that is eventually responsible for tip clearance noise. Further design parameters are compiled in Table 1. Two impellers with different diameters were manufactured, providing a variation of tip clearance; one with a large tip clearance ratio s/D_a = 1.0% (i.e. a clearance of 3 mm) and one with an extremely small gap of s/D_a = 0.1% (i.e. a clearance of 0.3 mm). Thin supporting struts were mounted one duct diameter downstream of the rotor, so that rotor/strut interaction was minimized, Figure 1 (right).

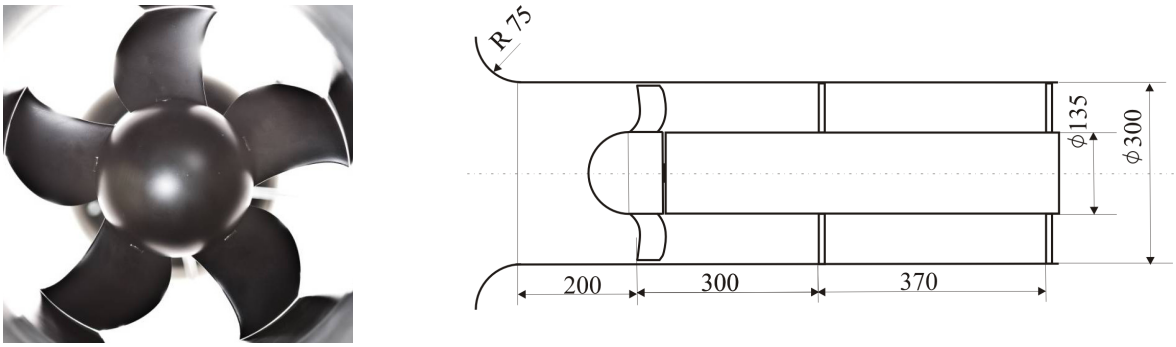

Figure 1: Manufactured impeller and fan assembly

Table 1: Important impeller design parameters

Duct diameter	D_a	[mm]	300	Design flow rate coefficient	ϕ	[-]	0.195
Hub to duct ratio	ν	[-]	0.45	Density of air	ρ	kg/m^3	1.2
Number of blades	z	[-]	5	Rotational speed	n	rev/min	3000

Aerodynamic and acoustic measurements and data evaluation

The aerodynamic fan performance was determined on a standard plenum test rig for fans according to the German standard DIN 24163. Being Δp_{ts} the total-to-static pressure rise and M the true rotor torque, the following non-dimensional fan performance coefficients are used - flow rate coefficient, total to static pressure rise coefficient, shaft power coefficient and total to static efficiency:

$$\phi = \frac{\dot{V}}{\frac{\pi^2}{4} D_a^{\,3} \cdot n}, \qquad \psi_{ts} = \frac{\Delta p_{ts}}{\frac{\pi^2}{2} \rho D_a^2 n^2}, \qquad \lambda = \frac{2\pi n M}{\frac{\pi^4}{8} \rho D_a^5 n^3}, \qquad \eta_{ts} = \frac{\dot{V} \Delta p_{ts}}{2\pi n M} \qquad (1 - 4)$$

The aeroacoustic investigations were carried out on a standardized acoustic duct test rig for fans with a semi-anechoic room (4.50 m×3.50 m×3.23 m) according to DIN ISO 5136, Figure 2. The impeller takes the air from a large semi-anechoic room and exhausts into a duct with an anechoic termination. The flow rate is controlled by a throttle downstream of the termination and is determined by a calibrated hot film probe in the duct.

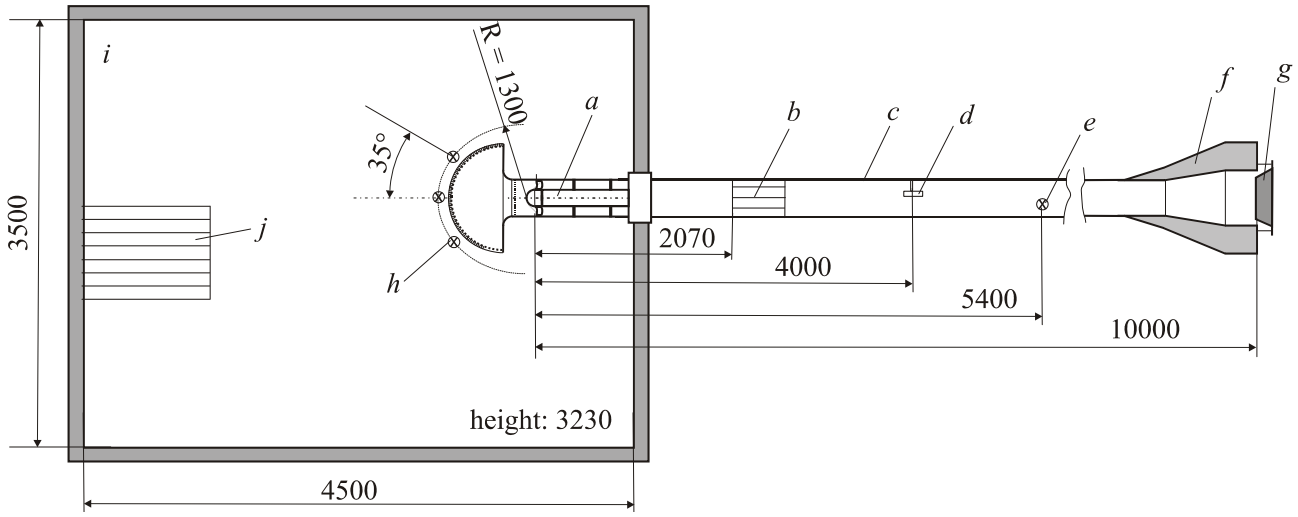

Figure 2: Duct test rig with semi-anechoic chamber (top view); (a) fan assembly (center line 1350 mm above reflecting ground), (b) star flow straightener, (c) duct, (d) induct microphone, (e) hot film mass flow meter, (f) anechoic termination, (g) adjustable throttle, (h) free field microphones, (i) semi-anechoic chamber, (j) air inlet grid on ground

The suction side sound pressure level L_{p5} (averaged through three microphones) is measured in the free field of the anechoic room by three microphones (Brüel & Kjaer, type 4190), placed on a hemispherical measurement surface around the inlet. All time signals were captured with a sampling frequency $f_{s\text{-}Exp}$ = 25.6 kHz. The spectral analysis is based on the power spectral density level (PSDL) which was obtained by the function *pwelch* in MATLAB® Vers. 7.11. The parameters chosen for *pwelch* were *window* = *hann(nfft)*, *noverlap* = 0, *nfft* = $fs \cdot T/n_{ave}$ (n_{ave}: number of averages). To make a fare comparison with the results from LBM, which has only relative short time signals, we choose T = 1 s of the total time record (10 s) from the experiment and obtain a frequency resolution of $\Delta f_{Exp} = fs/nfft = n_{ave}/T$ = 5 Hz (with n_{ave} = 5) in all spectra. For all levels, the reference pressure is $p_0 = 2 \cdot 10^{-5}$ Pa. All overall levels are the sum of narrow band levels from 100 Hz to 3 kHz (limited by the f_{max} in LBM-results, see equation 2).

NUMERICAL APPROACH

Lattice-Boltzmann-Method

To predict the unsteady flow phenomena associated with the tip flow and the generation and radiation of sound, a Lattice-Boltzmann-Method (LBM) is utilized. LBM-based methods are by nature explicit, transient and compressible. Unlike conventional CFD methods based on discretizing the macroscopic continuum equations, LBM starts from "mesoscopic" kinetic equations, i.e. the Boltzmann equation, to predict macroscopic fluid dynamics[18], [19]. The basic idea of LBM is to track the advection and collisions of fluid particles. Since the average number of particles in a representative volume of fluid far exceeds the compute power required to track them individually, the particles are grouped into a set of discrete *i*-directions. The computation follows the particle distribution function f_i which represents the number of particles in a unit of volume at a specific time and location moving with velocity c_i. As in statistical physics, the flow variables such as density and velocity are determined by taking the appropriate moments, i.e. summations over the set of discrete directions, of the particle distribution function.

In this study the commercial code PowerFlow™ in the version 5.0c is used. In order to model the effects of unresolved small scale turbulent fluctuations, in this code the Lattice-Boltzmann equation is extended by replacing its molecular relaxation time scale with an effective turbulent relaxation time scale derived from a systematic Renormalization Group (RG) procedure, see details in Chen et al. [20]-[22]. A turbulent wall-model, including the effect of pressure gradients, is also integrated into the solver. This method is called Very Large Eddy Simulation (VLES) and has been validated and used for several aeroacoustic problems[23]-[27]. The LBM scheme is solved on a grid composed of cubic volumetric elements, so called voxels, using a Variable Resolution (VR) strategy, where the grid size changes by a factor of two for adjacent resolution regions. For the simulations of flows in domains consisting of rotating and stationary regions, the computational domain is divided into a so called "body-fixed" Local Reference Frame (LRF) and a "ground-fixed" reference frame domain, connected by an interface, see details in Zhang et al.[28].

Numerical setup

The computational domain is the complete acoustic test rig from Figure 2 in full scale. For simplicity all inner walls of the semi-anechoic room (i.e. even the floor) are defined as porous. Both, air inlet and outlet region, are modeled as damping zones to avoid acoustic reflections. All other surfaces (nozzle, duct, fan impeller and fan hub) are specified as rigid walls. The mass flow according to the required fan operating point is specified at the inlet. Free exhaust at ambient atmospheric pressure is assumed at the outlet. The simulation is performed at the fan design point and a part load operating point, i.e. flow rate coefficient of 0.195 and 0.165 respectively. A LRF-domain around the rotating fan impeller is discretized using the finest grid resolution of Δx = 0.5 mm (VR10) corresponding to 600 voxels across the duct diameter. The large tip clearance is resolved with 6 voxels. It is showing that the aero-acoustic effect of large tip clearance can still be captured even with this relative coarse resolution. The small tip clearance is replaced by s/D_a = 0.0%, i.e. tip clearance is completely neglected. Later the comparisons of LBM predicted results to the experiment shows that this is an acceptable simplification. The VR-zones are denoted in Figure 3. The regions around the "microphone probes" are resolved spatially with Δx_{mic} = 8.0 mm (VR6). Assuming that the required number of points per wavelength to accurately capture acoustic waves is N_{ppw}=16 (Brès, G.A. et al.[29]), the maximum frequency f_{max} this grid solves is at the

$$f_{max} \sim \frac{c_0}{N_{ppw}\Delta x_{mic}} \sim 3 \text{ kHz} \qquad (2)$$

The LBM-results are evaluated using the data captured over an overall time interval $T_{sim} \approx 1$ s corresponding to approx. 50 impeller revolutions upon arriving a statistically stable fan operating

point, i.e. with settled flow rate and pressure rise. The simulation time step is Δt = 8.2·10^{-7} s in VR10. The data at the monitoring points in the acoustic far field, i.e. at the microphone probe positions, are captured with a sampling frequency $f_{s\text{-}Probe.}$ = 75822 Hz, the hydrostatic pressure fluctuations on the blade surface and in an adjacent annular volume with $f_{s\text{-}SurVol.}$ = 18955 Hz. All spectra are evaluated from the raw LBM data using the same method described in last section with same frequency resolution of Δf_{LBM} = 5 Hz.

The fan's overall pressure rise is evaluated in planes approx. one duct diameter up- and downstream from the fan impeller, area-averaged in each plane and time-averaged during ten revolutions. It was showing in the pre-study as a proper approach to archive the converged aerodynamic performances.

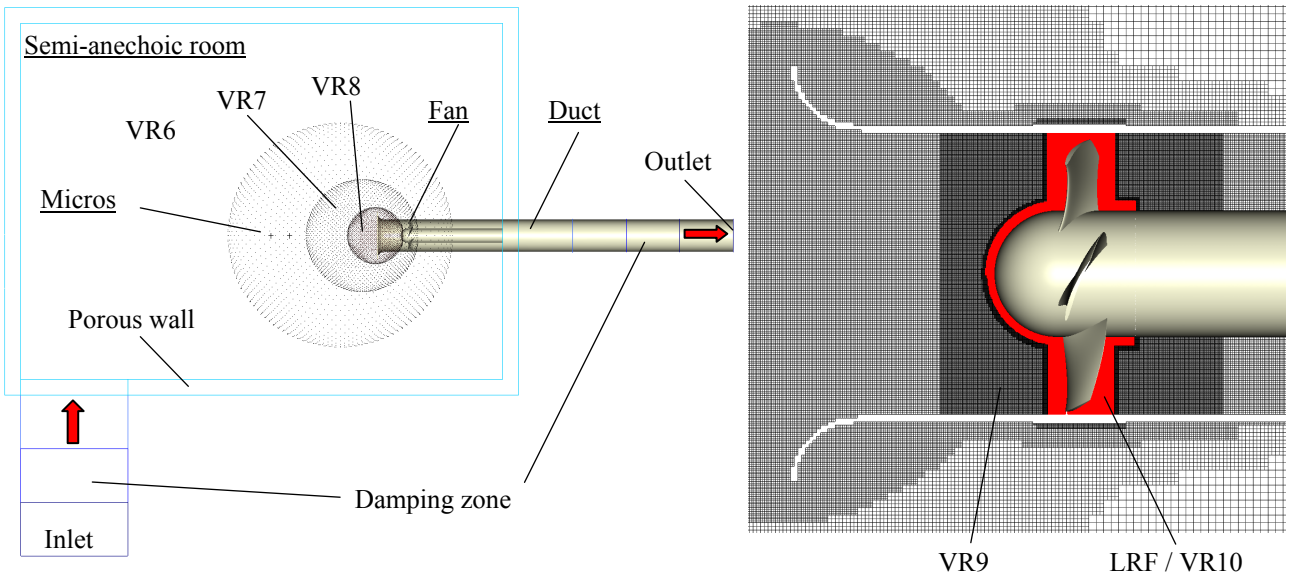

Figure 3: Simulation-domain including the semi-anechoic room and test rig duct (left), mesh detail in the fan section with LRF-domain (right, red)

RESULTS

Measured and LBM-predicted aerodynamic and acoustic overall characteristics

The aerodynamic overall performance characteristics in terms of ψ_{ts}, λ and η_{ts} as a function of ϕ are shown in Figure 4 (left). The effect of the tip clearance on the aerodynamic characteristics is rather obvious: Pressure rise and efficiency drop and the onset of stall moves to higher flow rates as the tip clearance is increased. The LBM-predictions at both design point and part load operation point are rather satisfactory.

The acoustic performance characteristics in terms of overall sound pressure level L_{p5} (up to 3 kHz) in the free field as a function of ϕ are shown in Figure 4 (right). With the small tip clearance the sound pressure level is nearly constant in the "healthy" flow regime down to the anticipated dramatic jump upon onset of stall, whereas for the large tip clearance the sound pressure level increases monotonically as the flow rate is decreased. The sound pressure as predicted from LBM reflects the effect of the tip clearance quite well: LBM and experiments show about 10 dB increase at design point and 15 dB at part load operating point due to the large clearance, although the absolute values are somewhat under predicted for the small tip clearance. This can be further discussed in the following.

The sound pressure spectra level in the free field are depicted in Figure 5, when the impellers are operated at their design and part load points. Both, measurements and LBM-prediction, show that the broadband sound is enhanced by increasing the tip clearance and decreasing the flow rate. Looking at the broadband components the agreement between experimentally determined and LBM

predicted spectra is satisfactory. The peaks at blade passing frequency (BPF) and its harmonics in the experiment results are very distinctive above the broadband level by the small tip clearance. This is not captured by the LBM simulation, which contributes to the lower overall sound pressure level comparing with the experiment. However, according to recent experimental investigations of the same fan/test rig assembly by Sturm and Carolus[30], BPF sound from this isolated axial fan is related to large scale inflow distortions caused by the slow flow in the room the fan takes its air from. Given the short physical simulation time of approximately one second it is clear that this slow flow in the room has not developed yet. At part load operating point by the large tip clearance there are several humps in certain narrow frequency bands with the center frequency of f_1= 175 Hz, f_2= 350 Hz and f_3= 525 Hz observed in the experiment and even in LBM predicted results this phenomenon is captured. The center frequency f_1= 175 Hz of the first narrow frequency band corresponds 70% of the BPF (250 Hz) and the f_2= 350 Hz and f_3= 525 Hz are the harmonics. This may be attributed to a similar mechanism observed by Magne et al.[15] and Piellard et al.[27].

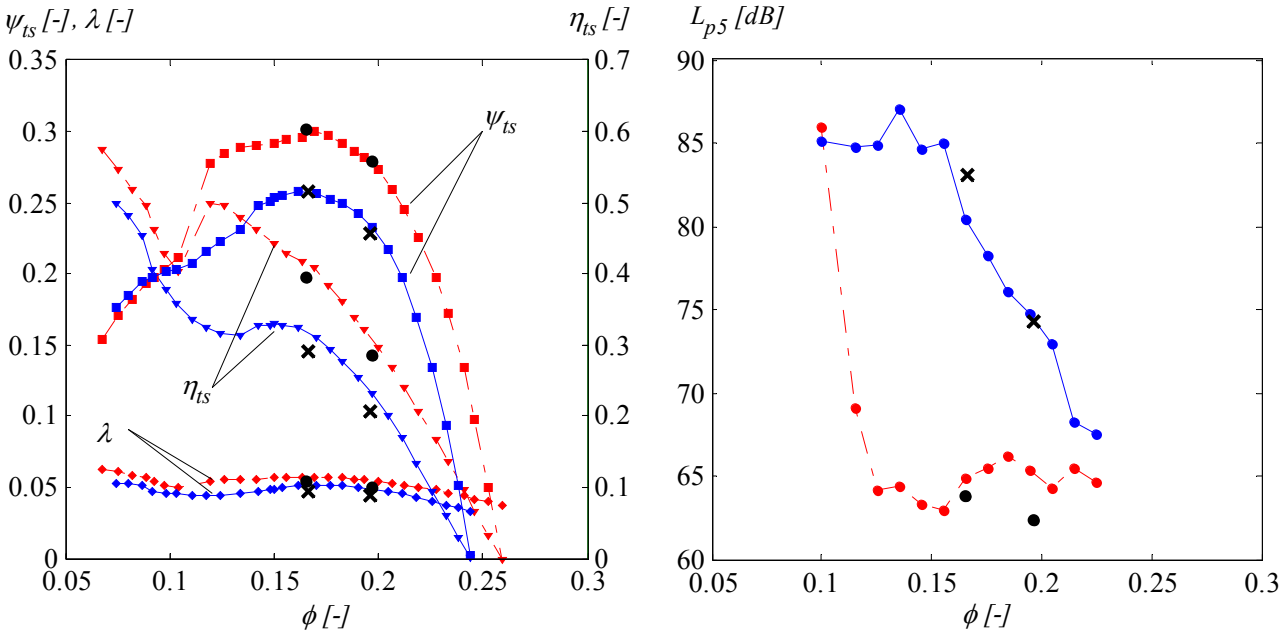

Figure 4: Aerodynamic characteristic (left) and acoustic (right) characteristics.

Red (Blue): Experiment - s/D_a = 0.1% (1.0%); Black dot (cross): LBM - s/D_a = 0.0% (1.0%)

LBM-predicted flow and acoustic field

It is an inherent advantage of any numerical field method that all overall quantities are derived from basic flow or acoustic field variables. Here, the satisfactory agreement of the LBM-predicted overall results encourages to analyze the LBM-predicted flow field in more detail. In the following paragraphs we will focus on unsteady phenomena at part load operating point with a flow rate coefficient ϕ= 0.165.

The instantaneous vortex structures are visualized by using isosurface of λ_2 colored by vorticity magnitude, Figure 6. In the case without tip clearance only vortex structure induced from the flow separation at the trailing edge can be captured, whereas due to the large tip clearance much more complex tip clearance vortices is observed. The large tip vortex structures with higher vorticity magnitude (red colored) separate to small vortex structures with lower vorticity strength through the blade passage and a strong interaction with the blade surface in vicinity of the tip can be expected. It shows a similar observation as in the study by Zhu and Carolus[13] using conventional unsteady CFD simulation but more detailed small scale vortex structures are captured here employing LBM.

Furthermore we will concentrate on the pressure fluctuation in the narrow frequency band between 150 and 200 Hz with center frequency of f_1= 175 Hz and the broad frequency band of f_4 between 1

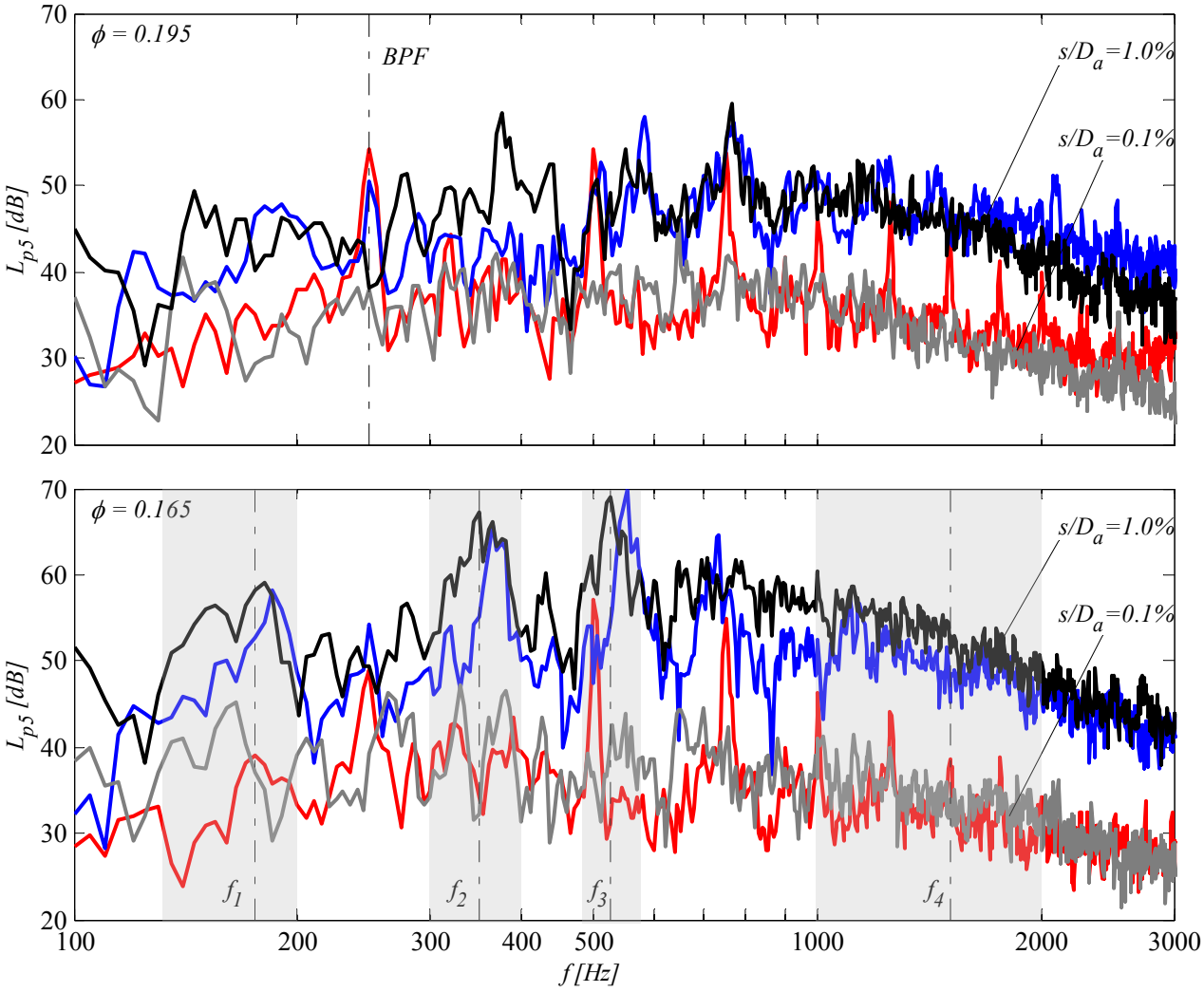

Figure 5: Sound pressure level spectra at design point (upper) and part load (lower), $\Delta f_{Exp} = \Delta f_{LBM}$ = 5 Hz.
Red (Blue): Experiment - s/Da = 0.1% (1.0%); Grey (Black): LBM - s/Da = 0.1% (1.0%)

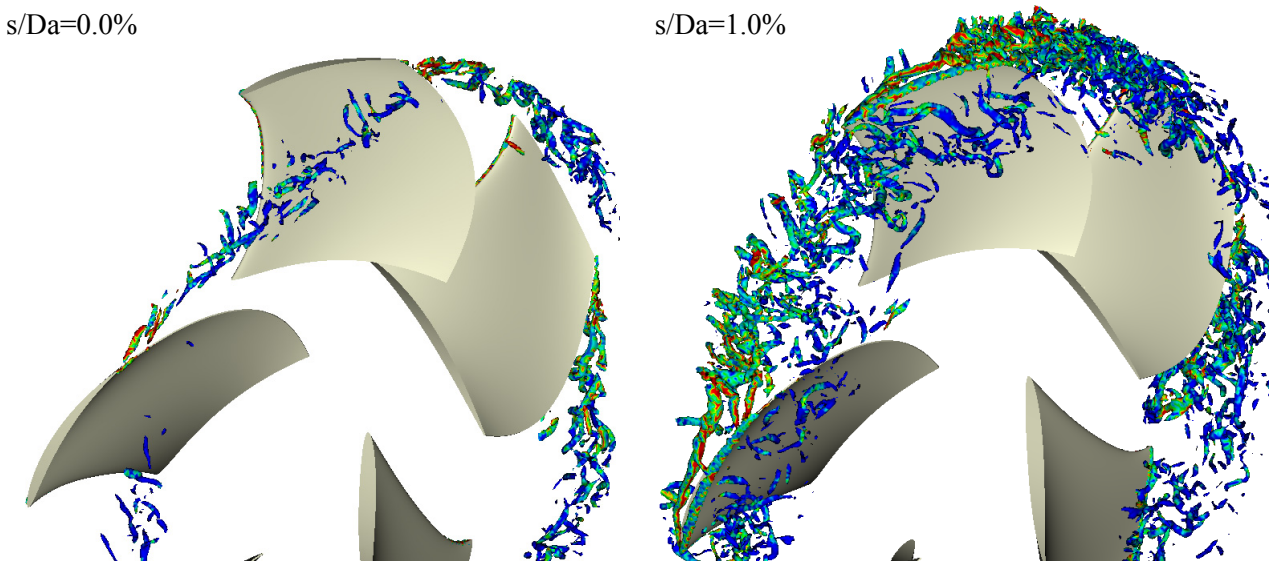

Figure 6. Instantaneous vortex structure illustrated with isosurface of λ_2 with value of -600 colored by voticity magnitude, ϕ=0.165

and 2 kHz, depicted in Figure 5. All flow patterns are constructed from band pass filtered data in these two frequency bands. For that the filtered signals are transformed back to the time domain employing a reverse Fast Fourier Transform. The respective instantaneous data over 10 impeller revolutions on the blade surfaces and in the flow field around the blade tips at an annular region only containing the upper half of the blades are captured.

The isosurfaces of power spectral density level of pressure fluctuations filtered in frequency band f_1 and f_4 with level 120 dB (grey) in the blade passages are depicted in Figure 7. In narrow frequency band f_1 there is no high level pressure fluctuation detected in the flow field near the blade tip in the case without tip clearance, whereas by the large tip clearance high level pressure fluctuation is observed at leading edge and on the suction side at blade tip. This region corresponds well where the large tip vortex structures with high vorticity strength are captured (Figure 6). In the frequency band between 1 and 2 kHz the separated small vortex structures due to the large tip clearance induce high pressure fluctuation level covering the whole blade passage, similar as observed at design point in Zhu et al.[16], but with stronger interaction with blade surfaces both on suction and pressure sides. Without tip clearance there is only small range of high pressure fluctuations induced from the separation flow from the trailing edge, which do not have obvious effect of the pressure field on the blade surfaces.

As a consequence there are areas of the blade surfaces contaminated by excessive pressure fluctuations. The small area of contamination in the hub region close to the trailing edge is independent of the tip gap. This gives a hint that the sound generated both in the narrow and broad frequency band f_1 and f_4 may be associated with vortex induced pressure fluctuations, respectively in the near of leading edge and on suction side or in the whole blade tip region. For the narrow frequency bands f_2 and f_3 similar results can be observed (not showing here).

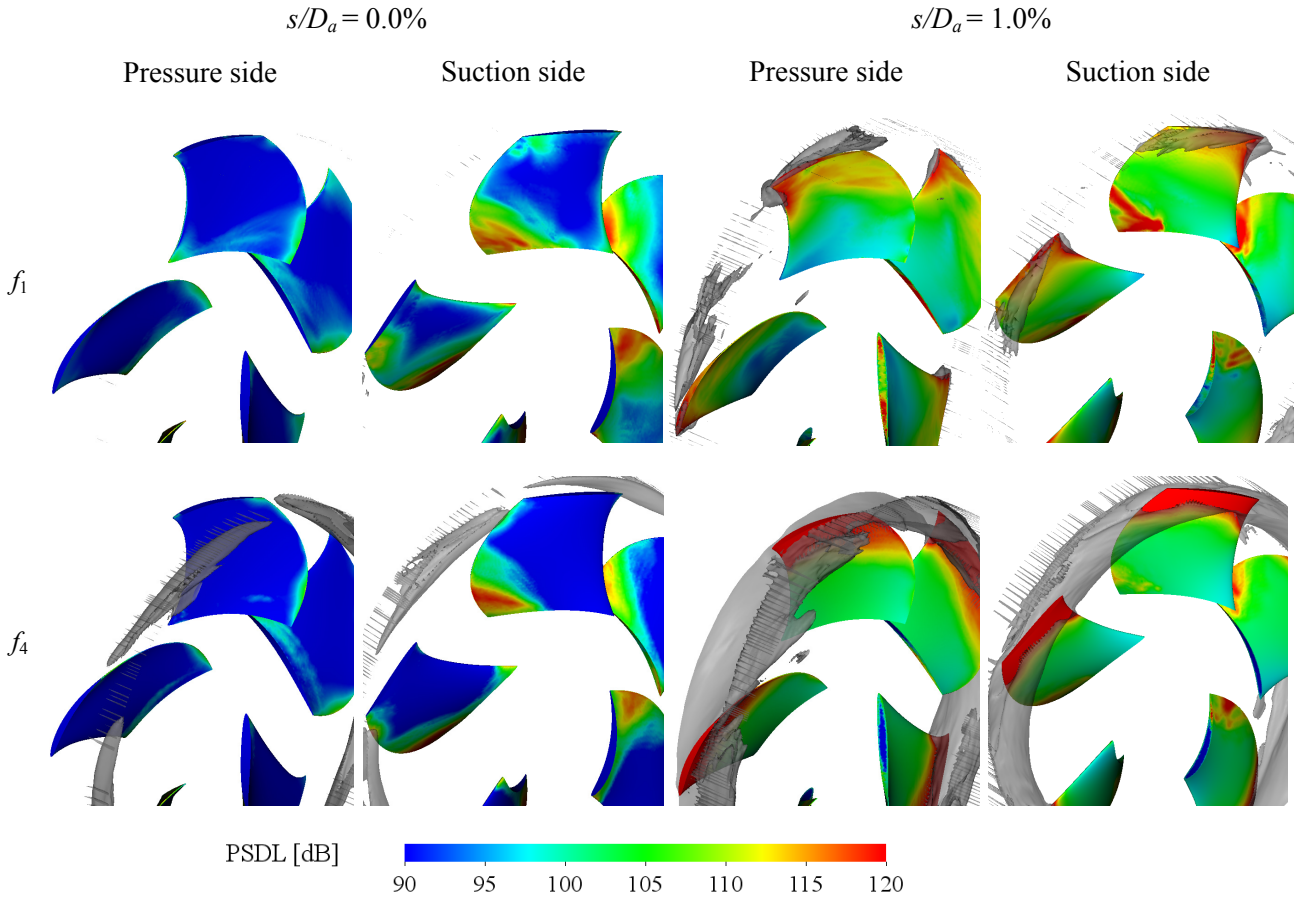

Figure 7. Power spectral density level of pressure fluctuations filtered in frequency band f_1 and f_4: on the blade surfaces and isosurface of level 120 dB (grey) in the blade passage, ϕ=0.165

The resulting field of instantaneous acoustic pressure far upstream of the impeller is depicted in Figure 8, as before in the narrow and broad frequency band f_1 and f_4. It is worth mentioning that exclusively the pressure in the stationary frame is visualized, not in the rotationary domain. Without tip clearance the monitoring points Microphone 1 to 3 only see quite weak waves propagating into the far field, whereas with the large tip clearance much stronger acoustic pressure fluctuations arrive at these monitoring points. This corresponds well with the sound pressure spectra from Figure 5. A time series of such instantaneous pictures could be used to visualize sound waves propagating from the impeller through the nozzle to the far field.

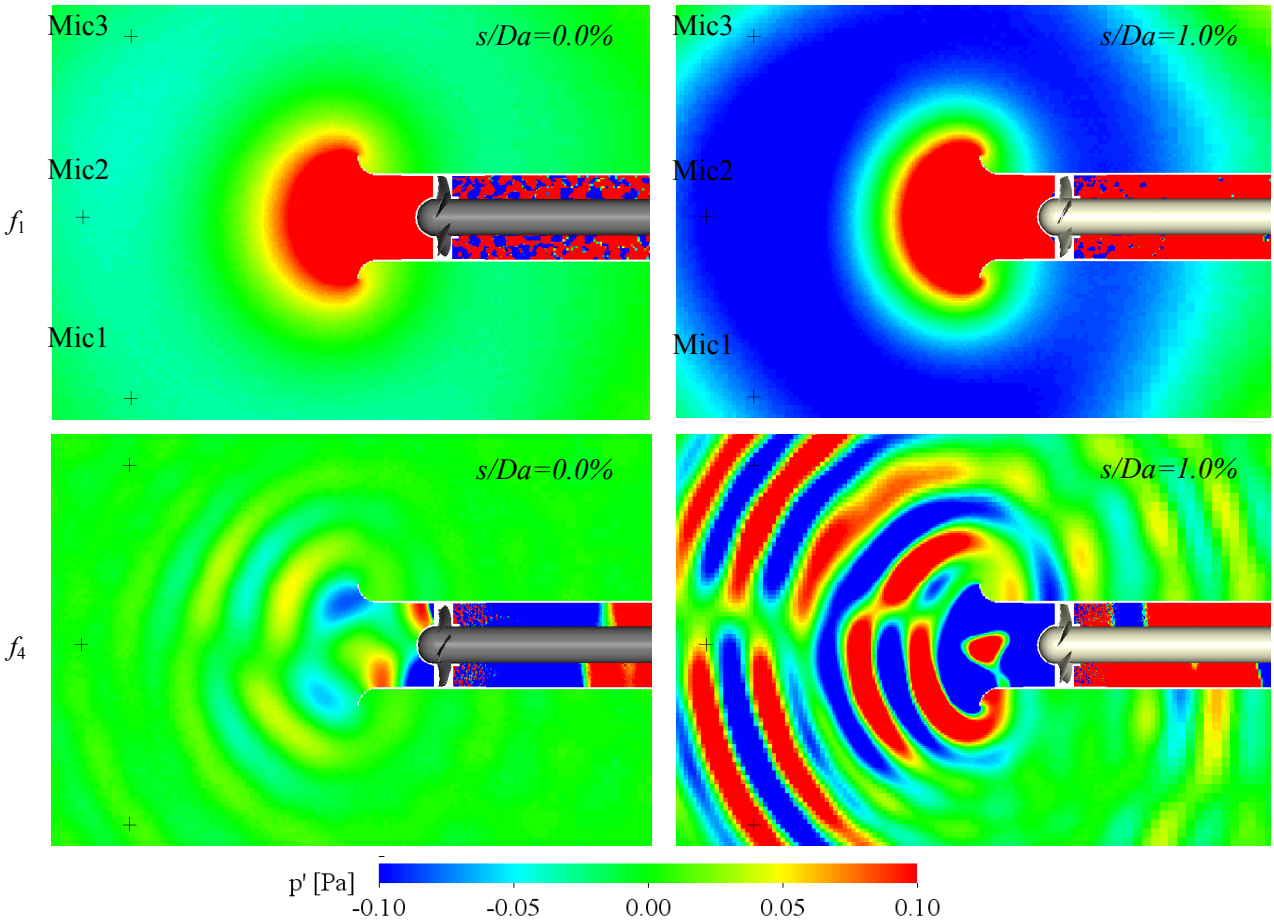

Figure 8: Instantaneous pressure fluctuation radiated to the far field filtered in frequency band f_1 and f_4., ϕ=0.165

CONCLUSIONS

The LBM-predicted flow and acoustic field in the vicinity of an axial fan impeller's tip gap revealed important details of the sound generating mechanism. A large tip clearance is responsible for a complex vortex system with a considerable degree of inherent unsteadiness. The consequences are fluctuations of static pressure in the flow field in the adjacent tip region and on the blade surfaces, both in the narrow and broad frequency bands. Those pressure fluctuations generate sound that is then radiated away from the complete impeller upstream into the free field with the typical hemispherical directivity pattern. Overall aerodynamic and acoustic fan performance data as predicted with the LBM were validated with experimental data. The agreement was satisfactory which justified looking at the LBM-predicted field data in detail. It would be of further value to validate "intermediate" quantities such as the surface pressure fluctuations on the stationary and rotating surfaces in the tip region, i.e. the acoustic sources themselves. Furthermore, running simulations for a longer physical time to capture longer transient data for the correlation analysis,

could be of great value for further understanding of tip clearance noise in the narrow frequency band.

ACKNOWLEDGEMENTS

The authors gratefully acknowledge the great support and assistance from Franck Pérot from Exa Corporation, Brisbane, CA, USA. The study was partly funded by the German Federal Ministry of Economics and Technology (BMWi) via the consortium for industrial research "Otto von Guericke" (AiF) and the Forschungsvereinigung Luft- und Trocknungstechnik e.V. (FLT).

BIBLIOGRAPHY

[1] Longhouse, R. E., *Control of Tip-Vortex Noise of Axial Flow Fans by Rotating Shrouds*, Journal of Sound and Vibration, 58, pp. 201-214, **1978**.

[2] You, D., Wang, M., Moin, P., and Mittal, R., *Large-Eddy Simulation Analysis of Mechanisms for Viscous Losses in a Turbomachinery Tip-Clearance Flow*, Journal of Fluid Mechanics, 586, pp. 177-204, **2007**.

[3] You, D., Wang, M., Moin, P., and Mittal, R., *Effects of Tip-Gap Size on the Tip-Leakage Flow in a Turbomachinery Cascade*, Physics of Fluids, 18(10), pp. 105:102-114, **2006**.

[4] Fukano, T., and Jang, C.-M., *Tip Clearance Noise of Axial Flow Fans Operating at Design and Off-Design Condition*, Journal of Sound and Vibration, 275, pp. 1027-1050, **2004**.

[5] Grilliat, J., Jacob, M. C., Camussi, R., and Caputi Gennaro, G., *Tip Leakage Experiment - Part One: Aerodynamic And Acoustic Measurements*, Proc. 13th AIAA/CEAS Aeroacoustics Conference, **2007**.

[6] Jacob, M. C., Grilliat, J., Camussi, R., Caputi Gennaro, G., *Aeroacoustic Investigation of a Single Airfoil Tip Leakage Flow*, International Journal of Aeroacoustics, 9(3), pp. 253-272, **2010**

[7] Kameier, F., and Neise, W., *Rotating Blade Flow Instability as a Source of Noise in Axial Turbomachines*, Journal of Sound and Vibration, 203, pp. 833-853, **1997**.

[8] März, J., Hah, C., and Neise, W., *An Experimental and Numerical Investigation Into the Mechanisms of Rotating Instability*, Journal of Turbomachinery, 124, pp. 367-375, **2002**.

[9] Neuhaus, L., and Neise, W., *Active Flow Control to Reduce the Tip Clearance Noise and Improve the Aerodynamic Performance of Axial Turbomachines*, Proc. Fan Noise 2003, p. 8, **2003**.

[10] Corsini, A., Rispoli, F., and Sheard, A. G., *Aerodynamic Performance of Blade Tip End-Plates Designed for Low-Noise Operation in Axial Flow Fans*, Journal of Fluids Engineering, 131(8), pp. 081101:1-13, **2009**.

[11] Aktürk, A., and Camci, C., 2010, *Axial Flow Fan Tip Leakage Flow Control Using Tip Platform*, Journal of Fluid Engineering, 132, **2010**.

[12] Aktürk, A., and Camci, C., *Tip Clearance Investigation of a Ducted Fan Used in VTOL UAVS Part 2 Novel Treatments vis Computational Design and Their experimental Verification*, Proc. ASME Turbo Expo, **2011**.

[13] Zhu, T., and Carolus, T. H., *Experimental And Unsteady Numerical Investigation of the Tip Clearance Noise of an Axial Fan*, ASME 2013 Turbine Blade Tip Symposium & Course Week, Hamburg, Germany, **2013**.

[14] Moreau, S., *Numerical Methods for the Prediction of Fan Aerodynamic and Acoustic Performances - Where are we today?*, Fan 2012, Senlis, France, **2012**.

[15] Magne, S., Sanjosé, M., Moreau, S., and Berry, A., *Aeroacoustic Prediction of the Tonal Noise Radiated by a Ring Fan in Uniform Inlet Flow*, 18th AIAA/CEAS Aeroacoustics Conference, **2012**.

[16] Zhu, T., Sturm, M., Carolus, T. H., Neuhierl, B., and Pérot, F., *Experimental and Numerical Investigation of Tip Clearance Noise of an Axial Fan Using a Lattice Boltzmann Method*, The 21st International Congress on Sound and Vibration, **2014**.
[17] Carolus, T. H., *Entwurfsprogramm für Niederdruckaxial-ventilatoren dAX-LP*, **1987 - 2014**.
[18] U. Frisch, B. Hasslacher and Y. Pomeau, *Lattice-Gas Automata for the Navier‐Stokes Equations*, Phys. Rev. Lett., 56, 1505-1508, **1986**.
[19] Guo, Z., Zhen, C. and Shi, B., *Discrete Lattice Effects on the Forcing Term in the Lattice Boltzmann Method*, Phys. Rev. E., 65, 046308, **2002**.
[20] Chen, H., Kandasamy, S., Orszag, S., Shock, R., Succi, S. and Yakhot, V., *Extended Boltzmann Kinetic Equation for Turbulent Flows*, Science, 301, pp. 633-636, **2003**.
[21] Chen, H., Orszag, S., Staroselsky, I. and Succi, S., *Expanded Analogy between Boltzmann Kinetic Theory of Fluid and Turbulence*, J. Fluid Mech., 519, pp. 307-314, **2004**.
[22] Chen, H., *Volumetric Formulation of the Lattice Boltzmann Method for Fluid Dynamics: Basic Concept*, Phys. Rev. E., 58, pp. 2955-2953, **1998**.
[23] Pérot, F., Kim, M.-S., Moreau, S., Henner, M., and Neal, D., *Direct Aeroacoustics Prediction of a Low Speed Axial Fan*, 16th AIAA/CEAS Aeroacoustics Conference, **2010**.
[24] Kim, M.S., Pérot, F., Meskine, M., *Aerodynamics and Acoustics Predictions of the 2-Blade NREL Wind Turbine using a Lattice Boltzmann Method*, 14th International Symposium on Rotating Machinery, **2012**.
[25] Pérot, F., Mann, A., Kim, M.S. and Fares, E., *Advanced Noise Control Fan Direct Aeroacoustics Predictions using a Lattice-Boltzmann Method*, 17th AIAA/CEAS Aeroacoustic Conference, **2012**.
[26] Pérot, F., Kim, M.S., Le Goff, V., Carniel, X., Goth, Y. and Chassaignon, C., *Numerical Optimization of the Tonal Noise of a Backward Centrifugal Fan using a Flow Obstruction*, Noise Control Engr. J., 61(3), **2013**.
[27] Piellard, M., Coutty, B., Le Goff, V., Vidal, V., and Pérot, F., *Direct Aeroacoustics Simulation of Automotive Engine Cooling Fan System: Effect of Upstream Geometry on Broadband Noise*, 20th AIAA/CEAS Aeroacoustics ConferenceAtlanta, GA, USA, **2014**.
[28] Zhang, R., Shan, X. and Chen, H., *Efficient Kinetic Method for Fluid Simulation Beyond Navier-Stokes Equation*, Phys. Rev. E., 74, 046703, **2006**.
[29] Brès, G.A., Pérot, F., Freed, D., *Properties of the Lattice-Boltzmann Method for Acoustics*, AIAA 2009-3395, , 13th AIAA/CEAS aeroacoustics conference, **2009**.
[30] Sturm, M., and Carolus, T. H., *Tonal Fan Noise of An Isolated Axial Fan Rotor Due to Inhomogeneous Coherent Structures at the Intake*, Noise Control Engineering Journal, 60(6), pp. 699-706, **2012**.